Magnetocrystalline anisotropy of nickel

Edwards, J.B.

MAGNETOCRYSTALLINE ANISOTROPY

OF

NICKEL

by

J.B. EDWARDS, B.Sc.

Presented in Candidature for the Degree of

Master of Science

1978.

SUMMARY

An attempt was made to measure the first three anisotropy constants of nickel from liquid helium temperature to room temperature, by the method of torque magnetometry. One crystal was used in the experiment: a small disc with flat surface as the (110) plane.

K_1 was found to be in agreement with the results of other workers; values of K_2 were found to be similar to those of other workers; measurements of K_3 were found to be highly unreliable.

In a second, and separate, investigation; the values of K_1 were measured in the (100) plane after a spherical crystal had been irradiated in an isotropic fast neutron flux of about 10^{18} neutrons/cm^2. The measured values were compared with those of another worker to observe any change in anisotropy due to irradiation. No significant change was detected.

The residual resistivity of nickel subject to the irradiation was also monitored, and compared to measurements made before irradiation. No significant change was found in the measurements.

CONTENTS

Chapter I

Introduction to Magnetocrystalline Anisotropy

The work required to magnetize a ferromagnetic crystal in a given direction depends upon that direction. This phenomenon is known as magnetocrystalline anisotropy. It is found experimentally that in the case of nickel (which has a face centred cubic structure) the crystallographic directions requiring least work to produce a given magnetization (not necessarily, but conveniently, the saturation magnetization) are the ⟨111⟩, or body diagonals of the unit cell. The directions requiring most work are the ⟨100⟩ or edges of the unit cell; whilst the face diagonals, or ⟨110⟩, require a work value between the other two. In the literature, these directions are referred to as "easy" and "hard" directions of magnetization.

If a co-ordinate system is set up such that the orientation of the magnetization is described by direction cosines with respect to the crystallographic axes, a phenomenological expression for the relationship between the potential energy of the magnetization and its orientation may be derived.

This expression takes into account the fact that this potential energy depends on the symmetry of the crystal. Thus to make the anisotropy energy independent of the sign of the direction cosine value, only even powers of the cosines are allowed; cross multiplications are not allowed; the anisotropy must be independent of any interchange of direction cosines.

If the direction cosines are as depicted in Fig. 1,1,

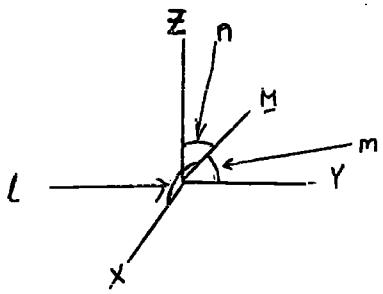

Fig. 1,1 THE DIRECTION COSINES (l,m,n) OF AN ARBITRARILY ORIENTATED VECTOR

then the anisotropy energy expression may be written in the form

$$E_A = K_o + K_1 (l^2m^2 + m^2n^2 + n^2l^2) + K_2 (l^2m^2n^2) + K_3 (l^2m^2 + m^2n^2 + n^2l^2)^2 + \ldots . \qquad (1,1)$$

in which $K_i = K_i (T)$ $\quad i = 1, 2, 3 \ldots$

To evaluate the K_i, the orientation of the magnetization is described in spherical polar co-ordinates and the direction cosines are transformed into the new co-ordinates. See Fig. (1,2).

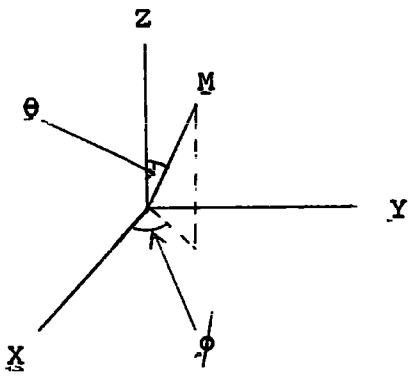

Fig.(1,2) SPHERICAL POLAR CO-ORDINATE SYSTEM

The relationship between the direction cosines and the spherical polar angles are:-

$$l = \frac{x}{r} = \frac{r \text{ Sin } \theta \text{ Cos } \phi}{r} = \text{Sin } \theta \text{ Cos } \phi \qquad (1,2a)$$

$$m = \frac{y}{r} = \frac{r \text{ Sin } \theta \text{ Sin } \phi}{r} = \text{Sin } \theta \text{ Sin } \phi \qquad (1,2b)$$

$$n = \frac{z}{r} = \frac{r \text{ Cos } \theta}{r} = \text{Cos } \theta \qquad (1,2c)$$

Following Brailsford (1966), we insert these results into (1,1) and the following is obtained:-

$$E_A = \frac{K_1}{64}\left((3 - 4\cos 2\theta + \cos 4\theta)(1 - \cos 4\phi) + 8(1 - \cos 4\theta)\right)$$

$$+ \frac{K_2}{256}(2 - \cos 2\theta - 2\cos 4\theta + \cos 6\theta)(1 - \cos 4\phi)$$

$$+ \frac{K_3}{64^2}\left((3 - 4\cos 2\theta + \cos 4\theta)(1 - \cos 4\phi) + 8(1 - \cos 4\theta)\right)^2 \qquad (1,3)$$

This expression is valid for any orientation in any cubic crystal.

To determine the relationship between the K_i in order that the $\langle 111 \rangle$ directions will have the lowest energy, the energy relationship is evaluated along the three directions $\langle 100 \rangle$, $\langle 110 \rangle$ and $\langle 111 \rangle$. This involves substituting the direction cosines into equation (1,1).

For $\langle 100 \rangle$ $l = 1$, $m = 0$, $n = 0$;

therefore, $E_A = 0$.

For $\langle 110 \rangle$ $l = \frac{1}{\sqrt{2}}$, $m = \frac{1}{\sqrt{2}}$, $n = 0$;

therefore, $E_A = \left(\frac{1}{\sqrt{2}}\right)^2 \left(\frac{1}{\sqrt{2}}\right)^2 K_1$

i.e. $E_A = \frac{K_1}{4}$

For $\langle 111 \rangle$ $l = \frac{1}{\sqrt{3}}$, $m = \frac{1}{\sqrt{3}}$, $n = \frac{1}{\sqrt{3}}$;

therefore, $E_A = \left[\left(\frac{1}{\sqrt{3}}\right)^2 \left(\frac{1}{\sqrt{3}}\right)^2 + \left(\frac{1}{\sqrt{3}}\right)^2 \left(\frac{1}{\sqrt{3}}\right)^2 + \left(\frac{1}{\sqrt{3}}\right)^2 \left(\frac{1}{\sqrt{3}}\right)^2\right] K_1$

$$+ \left(\frac{1}{\sqrt{3}} \cdot \frac{1}{\sqrt{3}} \cdot \frac{1}{\sqrt{3}}\right)^2 K_2$$

i.e. $E_A = \frac{K_1}{3} + \frac{K_2}{27}$

For $\langle 111 \rangle$ to be a direction of minimum energy, and if K_1 may be either positive or negative;

$K_1 > 0$; $\frac{K_1}{3} + \frac{K_2}{27} < 0$; $K_2 < -9K_1$

$K_1 < 0$; $\frac{K_1}{3} + \frac{K_2}{27} < \frac{K_1}{4}$; $K_2 < \frac{27}{12}(3K_1 - 4K_1)$

$K_2 < -\frac{9K_1}{4}$

Torque Curves with field rotated in (110) plane

The (110) plane contains all three principal directions and if the magnetization is constrained to rotate in this plane it will experience charges of energy associated with movement between them. If the following co-ordinate system is used;

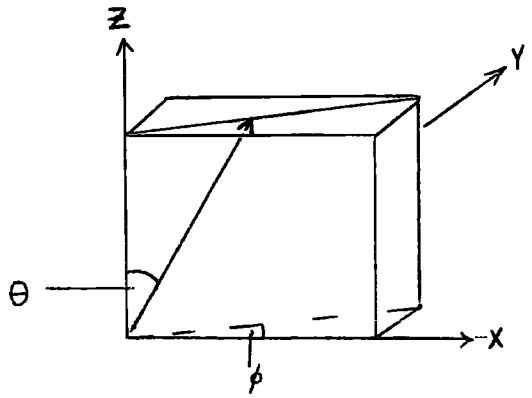

THE (110) PLANE

Fig. (1,3)

The plane depicted is a (1 $\bar{1}$ 0) plane which is equivalent to a (110) plane by symmetry of the cubic system. To obtain the energy equation in the (110) plane, ϕ is set to 45°. After collecting terms in cos nθ, the following is obtained;(from Equation 1,3)

$$E_A = -\left(\frac{K_1}{8} + \frac{K_2}{128} + \frac{11K_3}{256}\right) \cos 2\theta - \left(\frac{3K_1}{32} + \frac{K_2}{64} + \frac{17K_3}{512}\right) \cos 4\theta + \left(\frac{K_2}{128} + \frac{3K_3}{256}\right) \cos 6\theta \qquad (1,4)$$

Equation (1,4) then represents the anisotropy potential energy surface in the (110) plane.

In order to use the method of torque magnetometry to gain information about the anisotropy surface, the anisotropy energy equation is converted into an anisotropy torque equation. The work done, dE, in a small rotation, $d\theta$, by a torque, L, is:-

$$dE = Ld\theta$$

and, so for a magnetization vector lying on an anisotropy potential energy gradient, the anisotropy torque.

$$L_A = \frac{dE_A}{d\theta}$$

If this torque is balanced by an externally applied torque to produce equilibrium, this counter torque is equal to and opposite in sign to the above torque.

Differentiating (1,4) we obtain;

$$-\frac{dE_A}{d\theta} = -\left\{\frac{K_1}{4} + \frac{K_2}{64} + \frac{11K_3}{128}\right\} \text{Sin } 2\theta - \left\{\frac{3K_1}{8} + \frac{K_2}{16} + \frac{17K_3}{128}\right\} \text{Sin } 4\theta + \left\{\frac{3K_2}{64} + \frac{9K_3}{128}\right\} \text{Sin } 6\theta \quad (1,5)$$

This equation will henceforth be referred to as the (110) plane torque equation. For a discussion of Franse's (1969) torque equation, see Appendix III. The constants K_i have been measured in different planes, and by different techniques. The following investigations are of interest here:- Franse et al (1969), Amighian et al (1976), Gadsden et al (1977), Gadsden & Heath performed ferromagnetic resonance experiments on Nickel in the (110) plane, and obtained Values for the first 3 constants.

In the present work, an attempt was made to obtain K_i by the torque magnetometry method; I am indebted to Dr. Heath for the loan of one of their samples.

Torque Curves with field rotated in a (100) Plane

It is convenient to measure K_1 in the (100) plane for Nickel to attempt to observe changes in the anisotropy energy. The cause of these changes is discussed in Chapter 2.

To obtain a torque equation in the (100) plane, equation (1,3) is considered. With $\phi = 0$;

$$E_A = \frac{8K_1}{64}(1 - \text{Cos } 4\theta) + \frac{K_3}{64^2} 64 (1 - \text{Cos } 4\theta)^2$$

Differentiating to obtain the torque equation;

$$\frac{d E_A}{d \theta} = \frac{K_1}{2} \text{Sin } 4\theta + \frac{K_3}{8} \text{Sin } 4\theta - \frac{K_3}{16} \text{Sin } 8\theta$$

If to a first approximation, the terms in K_3 may be neglected,

$$L = \frac{K_1}{2} \quad \text{Sin } 4\theta \qquad (1,6)$$

This may be justified by observing the relative Values of K_1 and K_3 at 77K. Franse (1969) gives;

$$K_1 = -\ 84{\cdot}2 \times 10^3 \ Jm^{-3} \qquad K_3 = -\ 16{\cdot}4 \times 10^3 \ Jm^{-3}$$

so that K_1 is overestimated by about 5%, and the coefficient of Sin (8θ) is just over 2% of that of Sin (4θ).

The torque curves produced by rotating the field in the (100) plane may be used to evaluate K_1. This technique was used on two of Amighian's (1975) nickel spheres as described in Chapter 3.

Chapter 2

Theoretical Motivation

Review of the theory of Magneto Crystalline Anisotropy

The origin of anisotropy is believed to be a combination of Spin orbit coupling, and incomplete quenching of orbital angular momentum.

The theory is reviewed by reference to the main authors in the field.

Aukulov (1936) assumed that each spin had an intrinsic energy which depended on its direction, and which arises from the interaction between the spin and the internal magnetic field of the atom.

He showed; $$\frac{K_1(T)}{K_1(o)} \approx \left(\frac{M(T)}{M(o)}\right)^{10}$$

which applies only at temperatures such that;

$$\left(1 - \frac{M(T)}{M(o)}\right) \ll 1$$

Van Vleck (1937) suggested that anisotropy may result from indirect coupling between the spin moments of the nearest neighbours. The spin-orbit coupling would make the spins see the lattice through the electrostatic fields in the lattice.

Brooks (1940) applied a collective electron model. This model represents the exchange energy as a Weiss internal field; the spin orbit coupling perturbs this field. From the wave function used to describe the states of the 3-d electrons, a number of solutions may be found which correspond to the 5-fold degenerate 3-d electrons of the isolated atom. In the solid, 3-d orbitals are allowed to produce bands away from the other two, and an anisotropy energy may be calculated.

Using 4th order perturbation theory for a number of wave vector points over the Brillouin Zone and summing the spin orbit correction over all the occupied states, the correct order of magnitude for K_1 for nickel was obtained.

No strong temperature dependence of K_1 was found.

Fletcher (1954) followed Brooks with his own data (1952) for the d-band in nickel and got values of the anisotropy constants two orders of magnitude bigger than Brooks did.

Carr (1957) attempted to explain anisotropy by the coulomb energy only. He used a virial expansion and a perturbation. The anisotropy is due to the interaction between the charge distributed about a lattice site and the crystalline potential of the lattice.

Zener (1954) made two assumptions:-

a) the temperature dependence of the anisotropy arises solely from the local deviation in the direction of magnetization.

b) the local deviation in an elementary region is the sum of a very large number of independent deviations.

The local spin deviations could be represented by a "random walk function". Their affect on the magnetic anisotropy was expressed by representing the magnetic energy as a series of surface harmonics.

Zener arrived at a power law relationship for the coefficient C associated with the ℓ'th order harmonic;

$$\frac{C\ (T)}{C\ (o)} = \left(\frac{M_s(T)}{M_s(o)}\right)^{\ell(\ell+1)/2}$$

The right hand side of this equation was compared with the ratio K(T) /K(o), obtained from experiments on iron. Good agreement was found for $\ell = 4$ for K_1, and for $\ell = 6$ for K_2. In the case of nickel, the anisotropy decreases much more rapidly, and so Zener's classical assumptions would not be seen to be applicable.

Keffer (1955) re-examined Van Vleck's theory. He found that at low temperatures, pseudo-quadrupolar interactions would give a 10th power law; but as the temperature rose, a 6th power law - as for Van Vleck - came into force. This change can be seen to correspond to a change in the degree of correlation between neighbouring spins - a 10th power law from a high

correlation; a 6th power law from a low correlation. Keffer also re-derived the $\frac{\ell(\ell+1)}{2}$ generalization, due to Zener.

Brenner (1957) instead of using Zener's random walk function, he used a Boltzmann distribution, and found good agreement between theory and experiment for the first anisotropy constant (K_1) of nickel for the condition $\frac{T}{T_C} > 0.3$. He noted that the spin orbit coupling, due to increased lattice vibration and thermal expansion, might change the intrinsic shape of the anisotropy energy surface.

Carr (1958) used a Langevin function and adjusted it to fit the measured curve for magnetization against temperature, and from this obtained Zener's 10th power law. From Zener's results, and from the idea that the anisotropy surface varies with thermal expansion, Carr found agreement with experimental results for Cobalt. In the case of nickel, which has a cubic structure, he assumed that a 10th power law would be obtained; but, by using the thermal expansion idea developed for Cobalt, he included a factor to allow for lattice expansion.

$$K_1(T) = K_1(0,0)\left(1 - 1.74\frac{T}{T_C}\right)\left(\frac{M(T)}{M(o)}\right)^{10}$$

$K_1(0,0)$ is the anisotropy constant at $0^{o}K$ and under zero strain.

Van Vleck (1959) presented a Spin Hamiltonian, or effective potential, of the type $V = a(S_x^4 + S_y^4 + S_z^4) + C$. He discussed cubic anisotropy. C is included to average V to zero when the Zeeman components are equally weighted. By using this theory with high neighbouring correlation, Van Vleck found a 10th power law which was not applicable to nickel.

Keffer and Oguchi (1960) gave a physical picture of the origin of the dipolar type of interaction in the form of the precession of the spin vectors about the axis of quantization. Due to the strong correlation between their directions at low temperatures, they obtained a 10th power law.

Callen & Callen (1960) noted that the wide angular deviation of the individual spins from their average directions results in a decrease in anisotropy with increasing temperature. They assumed that the anisotropy surface does not change with temperature and at high temperatures the spins sample the surface over a wider angle, causing the measured anisotropy to decrease.

Callen & Callen (1966) used a quantum mechanical treatment to obtain an $\frac{\ell(\ell+1)}{2}$ low temperature law. The theory was extended to higher temperatures by using a Boltzmann distribution function for the spin deviation.

Aubert (1968) noted that, for nickel, the major contribution to magnetic anisotropy will be from the orbital contributions rather than the spin contributions. The spin-orbit interaction introduced anisotropy into the orbital contribution to energy and magnetization. He considered an effective field, H_S, collinear to M_S, and represented the interaction of the spin system on the quenched orbital moments through the spin-orbit interaction. He wrote:-

$M_L = aH_S + bH_S^2$ where M_L is the orbital contribution to magnetization.

Also, $W = -\frac{1}{2} aH_S^2 - \frac{1}{4} BH_S^4$

Where a is a constant, b depends on the direction of H_S and leads to the anisotropy of M_L.

$$H_S = -4\left(\frac{\Delta W}{\Delta M}\right) \quad ; \quad \Delta W = -\frac{1}{4} BH_S^2$$

$$\Delta M = BH_S^3$$

Wherein ΔW and ΔM are energy and magnetization differences between $\langle 111 \rangle$ and $\langle 100 \rangle$, B is the difference in b between the two directions. The model gives $H_S \propto M^{10}$.

Mori (1969) calculated values for K_1 and K_2 at low temperatures for the metals iron and nickel. Using a band structure due to Yamashita et al (1963), he showed that in those parts of the Brillouin Zone where the

orbital angular momentum was not quenched, the contributions to anisotropy were small. For temperature dependence he determined the splitting between plus and minus spin bands to agree with experimental results on temperature variation of magnetization and then recalculated K_1 & K_2 including the Fermi distribution. Agreement was not found for nickel.

Hausmann (1970) employed spin waves and ferromagnetic resonance phenomena to give a general derivation of the 10th power law for the constant K_1.

$$K_1 (T) = K_{1V} \left(1 - 10 \frac{(M(o) - M(T))}{M(o)} \right)$$

K_{1V} is the anisotropy constant in a state of vacuum of magnons.

Recent Magneto-Crystalline Anisotropy Background

Most theoretical models indicate that the first magneto-crystalline anisotropy constant of the transition metals is expected to vary as the 10th power of the magnetization. Expressed mathematically this is:-

$$\frac{K_1 (T)}{K_1 (O)} = \left(\frac{M(T)}{M(O)} \right)^{10}$$

Here, the magneto-crystalline anisotropy (hereinafter called anisotropy) is expressed in terms of K_1, which appears in the anisotropy energy equation, Eq. (1,1).

$$E_A = (\ell^2 m^2 + m^2 n^2 + n^2 \ell^2) K_1 + \ldots .$$

where ℓ, m, n are the direction cosines.

The relationship quoted above is found to be reasonably well obeyed by iron and cobalt, but not to be valid for nickel. Over some temperature ranges, in fact, K_1 is found to vary with magnetization up to its 70th power.

As theory and experiment are at variance over the description of this phenomenon, Franse et al (1968) suggested that the anomaly might be due to a link between the anisotropy and the mean free path of the conduction electrons, which is the average distance travelled by these electrons before they suffer scattering.

Attempts were made by several workers to control the variations in mean free path by the method of dilute alloying of the ferromagnetic anisotropic metal. Thus, Hausmann et al (1971) added molybdenum to nickel, and measured the anisotropy over a range of compositions for this alloy system. They found the following relationship between anisotropy for the alloy K_1^1 at a given temperature, and concentration.

$$K_1^1 (T,C) = K_1 (T) \exp (-\alpha C)$$

Where C is the concentration of the alloying material and K_1 (T) is exponential in (T). Since the concentration and temperature variables may be separated there is an indication that mean free path could play an important role in anisotropy.

Amighian & Corner (1975) added vanadium to nickel and measured both the anisotropy and mean free path of the system between 4.2°K & 300°K. They used a torque magnetometer for the anisotropy measurements and the mean free path variations were estimated from resistivity measurements. Their results were compared to those of Hausmann et al (1971), and it was found;

$$K_1 (T,C) = K_1 (0,C) \exp \left(-\frac{T}{T_o}\right)^x \qquad x = 1.49$$

$$K_1 (0,C) = K_1 (0,0) \exp (-\alpha C)$$

and $$\frac{K_1 (T)}{K_1 (0)} \propto \left(\frac{M(T)}{M(0)}\right)^n$$

in which n is temperature dependent, reaching a maximum at between 100 and 140°K. They found a small, but significant, anomaly in the resistivity of the alloys, but not for pure nickel in this region. (Amighian (1975)).

Amighian plotted a variable, α, derived from anisotropy measurements, against the atomic number of the impurity elements for a given at.% level in each case, having extrapolated the anisotropy to 0°K.

Following Farrell and Greig (1968), Amighian also plotted minority spin residual resistivity against atomic number. He found that, if he

chose different interpretations for minority spin residual resistivity for vanadium and titanium alloys, the two graphs were remarkably similar in shape.

It is possible that the act of alloying the materials will change the band structure from that of the pure metal, and so introduce a new variable. Low (1969) has used inelastic neutron scattering experiments to show that some alloys, which lie on the Slater - Pauling curve, have screening lengths of the order of 0•2 Angstroms. For these alloys, the magnetic disturbance is localized at the impurity atoms whilst for other alloys, the disturbance extends to first and second nearest neighbours. But the band structure changes may be small since anisotropy and minority spin resistivity measurements lie on similar smooth curves.

A different kind of magnetic disturbance to that produced by impurities may be produced by irradiating nickel with neutrons, with the intention of displacing the nickel atoms from their lattice sites and so creating scattering centres. Changes in conduction electron mean free path may be observed and measured through changes in the residual resistivity. If the anisotropy changes also, and if the change in anisotropy measured is comparable to the change which occurred when the nickel was alloyed to the same resistivity change as for the irradiated nickel, then the mean free path hypothesis would receive strong additional support.

PRINCIPLEOF THE TORQUE MAGNETOMETRY METHOD

When the crystal is magnetized in an arbitrary direction in the (110) plane, the crystal will attempt to align a $\langle 111 \rangle$ direction with the external field. By supplying an equal and opposite torque the crystal will be held in position against the anisotropy torque. This position will be one of equilibrium between the external torque and the anisotropy torque.

If the external field is now rotated in the (110) plane, it will force the magnetization to follow it, due to the M x H torque. When the magnetization travels across the plane it samples different portions of

the anisotropy energy surface and so feels different anisotropy torques. Thus, the external torque required to keep the crystal stable will vary, and measurement of this torque provides the means of measuring the K_i and hence determing the shape of the anisotropy energy surface. It should be emphasized at this point that the anisotropy torque is acting on the magnetization vector. This torque is correctly described in the (110) plane by the torque equation (1,5).

As mentioned above, however, the field torque, responsible for causing the magnetization to rotate, is described by the vector product M x H. This expression implies that the external field is not collinear with the magnetization. Now, whilst a theoretical torque curve expresses restoring torque as a function of the angle between the magnetization vector and a reference direction in the crystal, an empirical torque curve expresses restoring torque as a function of the angle between the external magnetic field and a reference direction in the crystal.

If the anisotropy torque is large, the magnetic field torque required to pull the magnetization round will also be large, and this will require a large value of M x H. In turn, this requires a large value of Sin δ $|\underline{M}||H|$ which implies a large value of δ (large relative to collinearity that is). On the other hand, if the anisotropy torque is small, the corresponding value of δ will be small.

This overall variation in the relative positions of magnetization and external field will cause mis-estimation of the position of the magnetization at which a given torque is being exerted - since we are in fact recording the position of the field at which a given torque is being exerted.

From the above arguments, it can be seen that the torque equation curve will be distorted in the experimental set up. It is important to see, for the (110) plane, how this relationship between external field and magnetization will distort the curve.

DETAILED DISCUSSION OF TORQUE CURVES

Consider the anisotropy energy diagram in the(110)plane, shown here with angle along a horizontal axis. See Fig. (2,1).

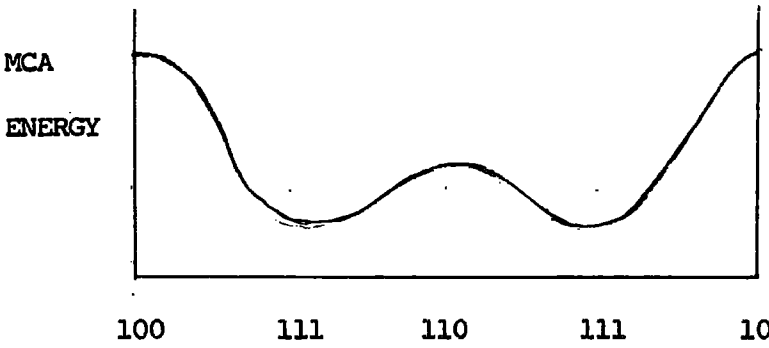

ANISOTROPY ENERGY DIAGRAM IN 110 PLANE

Fig.(2,1)

The anisotropy torque is given by - $dE_A/d\theta$ and has maximum value when on the steepest part of the energy curve. See Fig. (2,2).

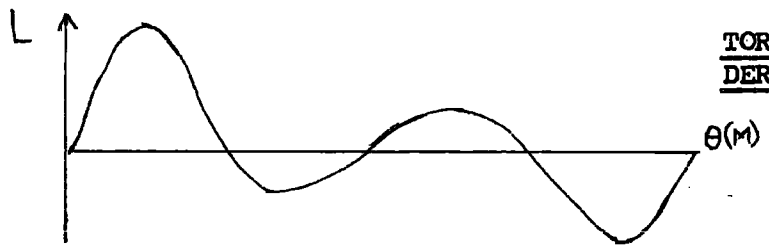

TORQUE CURVE IN 110 PLANE DERIVED FROM ABOVE

Fig.(2,2)

The applied counter torque employed to equalize the anisotropy torque to prevent the crystal moving will be a mirror image of this curve in the θ-axis.

If the external field is followed as it rotates in the (110) plane, it will be seen that the magnetization lies between the field and the $\langle 111 \rangle$ easy direction when the field is going from $\langle 100 \rangle$ to $\langle 111 \rangle$. Thus, during this traverse, the magnetization arrives at a steeper part of the energy gradient before the external field, and the associated magneto crystalline torque is higher than it would be if the magnetization were collinear with the external field. So for this position of external field, the torque is higher than for the corresponding magnetization torque curve.

Continuing the journey, the magnetization reaches the maximum slope position before the external field does, and since the torque is due to

interactions on the magnetization, the maximum torque will occur to the left of the peak shown on the $\theta(M)$ torque curve.

When the external field passes through the position of maximum slope, the magnetization lies on a position of lower slope and the crystalline torque is correspondingly less.

When the external field comes into line with the $[111]$ direction, it becomes collinear with the magnetization and the torques go to zero.

As the field starts to move from the $[111]$ to $[1\bar{1}0]$ directions, the anisotropy forces will tend to try to draw the magnetization back into the easy direction. Thus, the external field will arrive at the maximum slope position before the magnetization - in contrast to the previous case. Thus, the recorded torque will be less than that for the same position on the $\theta(M)$ torque curve. Only when the magnetization reaches the point of maximum slope, after the field has passed this point, will the maximum torque be shown. On the $[1\bar{1}0]$ direction, there will be a point where the field and magnetization are collinear, such that just after that point the magnetization can again assume a position between the external field and the nearest easy direction.

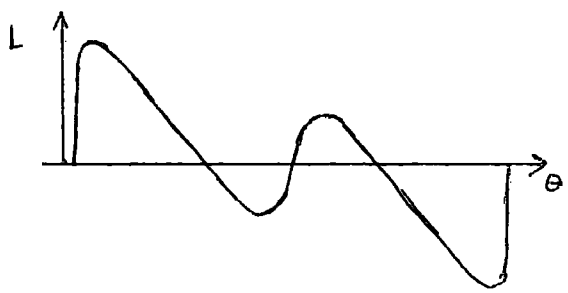

SHEARED TORQUE CURVE

Fig.(2,3)

The form of the resulting distortion on the curve is termed "shear". Without some magnitude of shearing, torque curves would be unobtainable in the present method. The shear was eliminated by projecting the torque curve through a suitably inclined graticule so that the points on the curve were displaced in the X -direction by an amount which would remove the

shear of the curve. By examining the geometrical relationship between the magnetization vector and the field vector, Welford (1974) arrived at an expression for the value of the shear. His argument is reproduced here:-

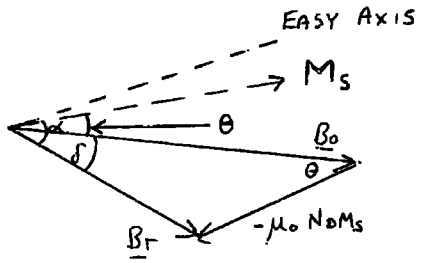

MAGNETIC VECTORS IN THE CRYSTAL

Fig.(2,4)

In the triangle; $\frac{B_r}{\text{Sin } \theta} = \frac{B_0}{\text{Sin } (180-(\theta + \delta))}$

$$B_r \text{ Sin } \alpha = B \text{ Sin } \theta$$

The magnetic torque per unit volume exerted by the field on the magnetization, and equal to the anisotropy torque is:-

$$\frac{L}{V} = \frac{B_r M_S \text{ Sin } \alpha}{\mu_0} \qquad M_S \text{ is the Saturation Magnetization}$$

$$= \frac{B_0 M_S \text{ Sin } \theta}{\mu_0}$$

$$\theta = \text{Sin}^{-1} \frac{\mu_0 L}{B_0 M_S V} \qquad (2,1)$$

In principle, the method of analysis was to perform a numerical Fourier analysis on the torque curves which were produced by the experimental arrangement described in Chapter 3. Then, the Fourier Coefficients so obtained could be equated to the Coefficients of Sin ($n\theta$) in equation (1,5). The resulting simultaneous equations are:-

$$32K_1 + 2K_2 + 11K_3 = 128A_2 \qquad (2,2)$$

$$48K_1 + 8K_2 + 17K_3 = 128A_4 \qquad (2,3)$$

$$6K_2 + 9K_3 = 128A_6 \qquad (2,4)$$

These were solved to yield the K_i in the (110) plane.

The whole calculation was performed by the Northumbrian Universities Multi-Access computer, using a programme written in Fortran IV (Formula-Translation). The programme is included in Appendix I

Chapter 3

Experimental Details

Anisotropy Measurements

Torque Magnetometer Apparatus

Fig. (3,1) depicts schematically the torque magnetometer. The crystal specimen is held vertically between two ligaments. A light beam falls on a small plane mirror in the suspended system and is reflected onto two photo-transistors. When there is no torque acting on the system, the beam is made to fall symmetrically on these and their currents are equal. If a torque is experienced by the suspended system, the light beam moves slightly and the currents become unequal. Two amplifiers feed a current proportional to the difference in photo transistor outputs to a counter torque coil which is mounted in the gap of a permanent magnet (not shown).

This servo system produces a counter torque which just balances the deflecting torque. A voltage proportional to the counter torque current is applied to the Y input on an X - Y recorder.

The torque on the sample is produced by the magnetic field due to an electromagnet which may be rotated and a voltage derived from a potentiometer on the electromagnet base is connected to the X-input of the recorder. This X - Y recorder can be used to trace a torque curve as detailed in Chapter 2.

Legend for Fig. (3,1)

A	Amplifier
B	Plane Mirror
C	Counter Torque Coil
D	Crystal Specimen
E	Electromagnet
F	Slide wire over transparent insulation on magnet scale
G	Sliding Contact
H	Rails on which magnet moves
J	Resistor
K	Voltage Supply
L	X - Y Recorder
M	Warning Meters
N,N'	Support Ligaments
PT1, PT2	Phototransistors
S	Projector Light Source
T	Concave Mirror
U	Output Potentiometer

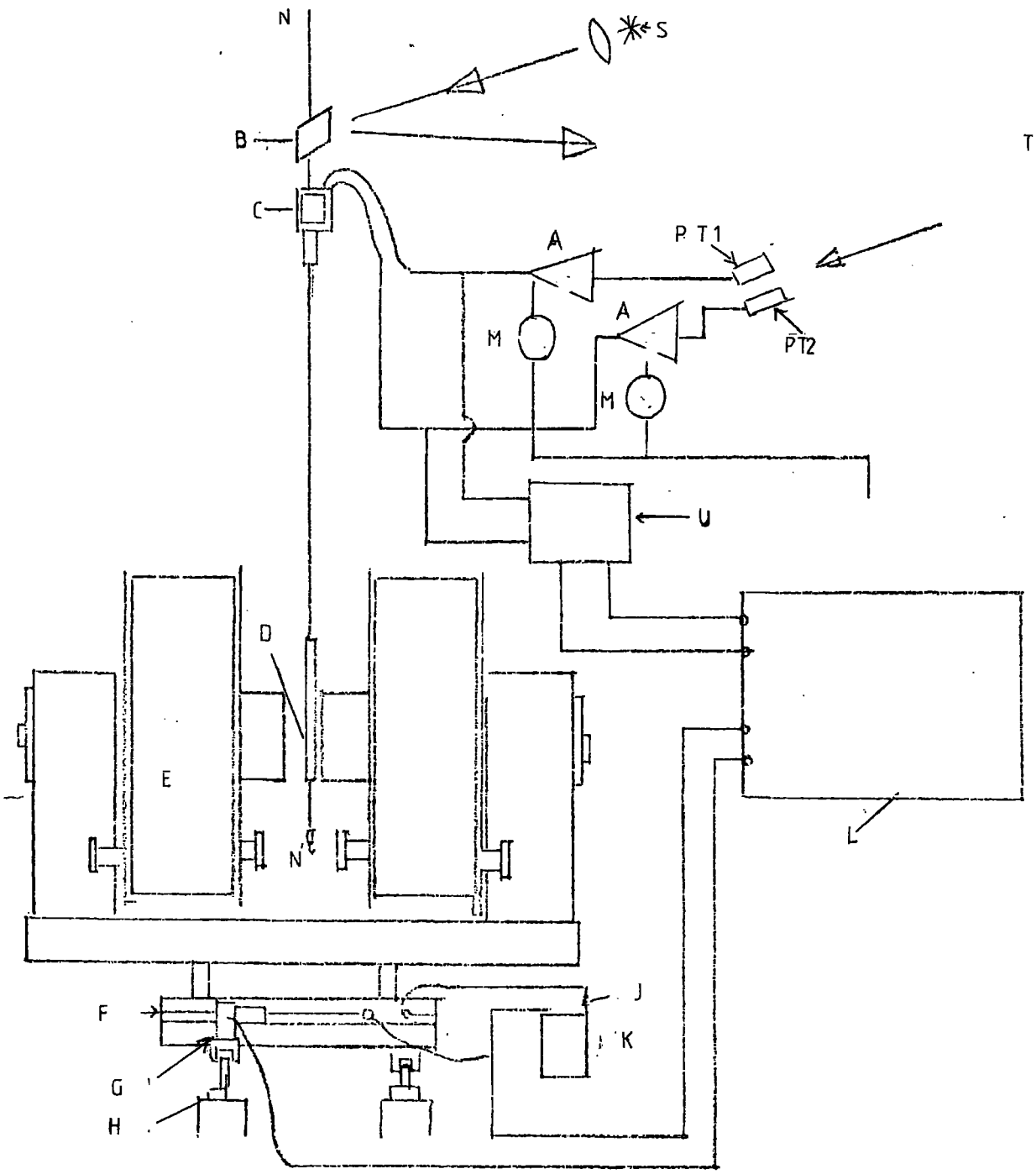

Fig. (3,1)

TORQUE MAGNETOMETER SCHEMATIC

Magnetometer Calibration

The apparatus was calibrated by the method used by Welford (1974). A small coil of N turns, each of cross sectional area A is attached to the magnetometer suspension around the specimen-holding volume, without the specimen being present. The coil is orientated so that its magnetic moment is normal to the field B of the electromagnet. Thus, when current I flows through both, a torque BANI is exerted on the test coil.

The magnetometer gave an output which was a measure of the torque on the test coil. The measurements were performed over a range of test coil currents, and over a range of electromagnet coil currents.

The result of the calibration gave:-

Calibration factor = 1.29×10^{-2} N m V^{-1}

Standard Deviation of 3.5×10^{-4} based on 14 readings.

This value was used to evaluate K_1 in the (100) plane, but a value of 1.24×10^{-2} N.M V^{-1} was used for K_1, K_2 and K_3 in the (110) plane, since these measurements (110) were carried out before those in the (100) plane, and it was thought that 1.24×10^{-2} more nearly represents the conditions pertaining at that time. Between the performance of the experiments, the magnetometer was dismantled several times, and this dismantling of the apparatus may have changed its calibration condition.

(110) Plane Specimen

The crystal disc was examined using the Laue technique to ensure that the (110) plane was indeed parallel to the surface of the disc. A molybdenum target tube was selected and the conditions chosen were; 26kV, 32 mA, 5 minutes exposure. The recording medium was a Polaroid type 57 film. The (110) plane was established to be the flat face of the disc to within 0.5°.

With the surface plane identified, the crystal was cleaned in alcohol, and weighed on an electronic balance and then measured using a micrometer. The specimen was attached to the magnetometer by means of a specimen holder, and the attachment was made by "Durofix" glue. The specimen was simply pushed on to the holder, thereby sandwiching a film of glue between the two. This action meant that the orientation of the crystallographic directions in the specimen were unknown, with a consequence that a torque curve exactly like those depicted in Chapter 1 were very unlikely to be obtained, the torque curves would in general have an arbitrary zero.

(100) Plane Samples

Consideration will be given here to the experimental techniques employed in testing the hypothesis mentioned in Chapter 2.

Four samples were irradiated; Amighian's 5N & 4N purity spheres and two rods, also of 5N & 4N purity, on which the resistivity checks could be performed. Since Amighian had previously measured the anisotropy and resistivity of these samples, their use provided a good datum from which to observe any changes incurred by radiation damage.

The samples (a sphere and a rod) were packaged in Cadmium sheet in one case, and in Cadmium foil and a polythene container in the other. They were subjected to an isotropic integrated dose of 10^{17} - 10^{19} fast neutrons/cm^2 by placing them in the centre of the swimming pool reactor at the AWRE Aldermaston.

The Cadmium foil was used to absorb thermal neutrons in the reactor. Nickel has a high capture cross section for thermal neutrons, and the results of such capture are not the displacement of the nickel atoms from the lattice sites. Indeed, the result of such capture is a nuclear reaction which renders the sample radioactive, and such radioactivity is undesirable. By excluding the thermal neutrons, only high energy neutrons

can bombard the crystals and cause the displacement of nickel atoms. Presumably, by this procedure, the activity resulting from the irradiation is kept low.

On returning from the AWRE the samples were placed in the radioactive store at Durham and left there for about a year. At this stage, the level of radiation was less than 1.5 mrem hr^{-1} based on a 40 hour continuous exposure week.

Legal requirements mean that the handling of radioactive materials in the laboratory be carried out under the supervision of the Radiation Protection Officer. A precise programme for the manipulation of the samples was written out, and this is given in Appendix I.

The samples were cleaned in analytical nitric acid by immersion. The orientation was performed using the Laue method. The crystal was stuck to a specimen holder by plasticine. The specimen holder was mounted in a goniometer jig which was designed to be able to move along two independent axes, and to rotate in planes perpendicular to these axes. The axes of rotation coincided at a point very near the centre of the specimen holder bracket, so that the crystal could be held in position coincident with the intersection of the two rotation axes. When the crystal was correctly mounted there would be no translatory motion when the goniometer was manipulated.

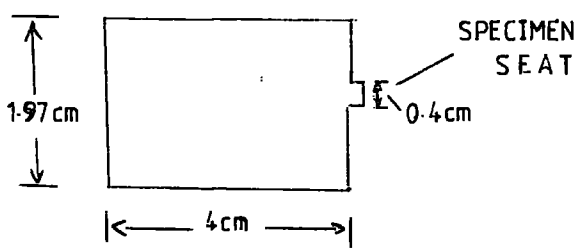

SPECIMEN HOLDER TO FIT IN GONIOMETER

Fig. (3,2)

The use of plasticine permitted the specimen holder to be stuck to the crystal rather than vice-versa which might have involved handling the crystal, which was undesirable.

With the crystal mounted in the X-ray beam, an exposure was made using 20 kV H.T., 20 mA tube current and a molybdenum target. Exposure times of about 5 minutes were found to be satisfactory. Polaroid type 57 film was used.

Photographs would show Bragg reflections appearing as white spots, and any particularly bright spots occurred at the intersection of two or more zones. The coordinates of such spots were measured on a Greninger chart, and the goniometer manipulated to bring the zone intersection spot into the centre of the film, in the hope that a pattern showing identifiable symmetry would be seen around the spot.

If no spots were found, or no brighter spots were found at the start, the crystal was moved abitrarily, and the "fishing" process continued until spots were found.

By searching out for the spot pattern symmetry in this way, the particular crystallographic direction which happened to be collinear to the X-ray beam could be identified. Knowing that the crystal was cubic, the angles between the planes are the same as the angles between the poles, so we may turn the crystal around according to the geometry of the crystal and so arrive at a correct orientation.

For the present purpose it was required to have the (100) spot in the centre of the film with a 4-fold symmetry of spots around it. When a Laue picture had been taken which showed this, the area of the crystal in the beam path was marked by a light touch of "Sno-pake" to label the pole in case of accident.

Then, the tufnol holder, which would attach the sphere to the magnetometer was placed in a spring holder which had a groove in its base so that it could rest on the X-ray arm which supported the crystal's goniometer. When the holder was so placed, Fig. (3,3) it caused the tufnol carrier to lie with its axis parallel to the arm; so, by adjusting the height of the goniometer, the crystal could be glued carefully and accurately

to the tufnol holder using "Evostick" glue. When the glue had set, the crystal on the tufnol holder was placed in the magnetometer.

The experimental procedure from here was closely similar to that for the Nottingham crystal, mentioned earlier.

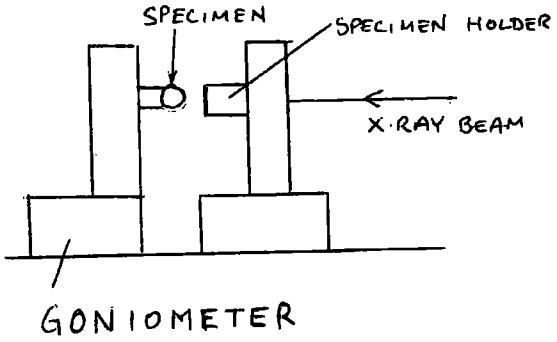

CRYSTAL TRANSFER ARRANGEMENT

Fig. (3,3)

Resistivity Measurements

Resistivity may be obtained from measurements of the resistance of a bar of known geometry. To obtain the variation of resistivity with temperature, the bar was placed in an Allbon Saunders cryostat. The cryostat had a long central column with a specimen holder at the bottom which could accommodate the bar. The holder had a semiconductor temperature sensor, Lakeshore cryotronics diode type DT-500KL, which took a current of 100 mA, and gave a temperature dependent voltage of between 2.1 V & 0.4 V corresponding to temps between 4.2°K & 300°K. The cryostat also had a heater fitted to allow intermediate temperatures to be attained.

A constant current was passed through the sample, and the voltage across a given pair of contacts was measured. The current was assumed uniform between the voltage contacts. If V is the voltage from these contacts, and I is the current between them;

$$\rho = \frac{AV}{I\ell} \quad \text{, where } \ell \text{ is the contact spacing} \qquad (3,1)$$

Amighian (1975) used a D.C. method to measure the resistivity of the samples, and a D.C. method was employed in this investigation also.

The surface of each bar was swabbed with analytical nitric acid solution to clean it. A small rectangle of fine gauge veroboard was cut to approximately 2 cm x 0.5 cm. Four 26 S.W.G. wires were passed through the board holes so that they protruded by about 0.5 cm above the non-metallic side of the board. In this position, they were soldered to the metallic side of the board. Using this relatively sturdy assembly, the wires on the plastic side of the board were spot welded to the sample bar so that two were close to each other at one end of the bar, and two were close to each other at the other end.

This procedure was found to be more reliable than spot welding before soldering. The spot welds were checked under a low power microscope to ensure that the welds had flowed. The welding conditions depend upon the

materials being welded and on the electrode materials, and information may be found with the equipment, situated in the Applied Physics building at Durham.

Insulated copper leads were soldered further down the veroboard strips from the S.W.G. leads; the insulated leads were taken to the head of the cryostat. The specimen and veroboard were glued by "Evostick" to the specimen holder - both to keep them in position and to prevent the metals coming into contact with the metallic specimen holder.

At frequent intervals in the execution of this procedure, continuity checks were made using an "Avo" meter.

The specimen holder was inserted into the cryostat and external connections were made. The current was measured using a 2 Amp F.S.D. ammeter; and the voltage was measured using a Solartron digital voltmeter (D.V.M.) reading to 1 μV.

Chapter 4

Results Analysis

The torque curves were analysed by numerical integration in a Fourier expansion.

In the simplest case, the torque curve would be as depicted in Chapter 2. However, as noted in that Chapter, the orientation of the $[100]$, $[111]$, and $[110]$ crystallographic axes was unknown; except that they lay somewhere in the plane of the disc. Also, since the output device - the pen recorder - was essentially a centre-zero analogue voltmeter, if the leads to it were connected in an arbitrary fashion, the curve would, at first sight, bear no resemblance to the required curve. The origin of the measured curve is displaced unpredictably and location of the true origin and subsequent angular correction is a tedious process. This may be avoided as follows:-

Equation (1,5) is:-

$$\frac{dE_A}{d\theta} = \left(\frac{K_1}{4} + \frac{K_2}{64} + \frac{11K_3}{128}\right) \text{Sin } 2\theta + \left(\frac{3K_1}{8} + \frac{K_2}{16} + \frac{17K_3}{128}\right) \text{Sin } 4\theta - \left(\frac{3K_2}{64} + \frac{9K_3}{128}\right) \text{Sin } 6\theta$$

This may be re-written:-

$$\frac{dE_A}{d\theta} = L_A = \sum A_n \text{Sin } n\theta$$

Due to the random orientation of the crystal, the empirical torque curve may be expressed by including an unknown phase,

$$L_A = \sum A_n \text{ Sin } (n\theta + \phi_n) \qquad (4,2)$$

A function may be expanded in a Fourier Series as follows:-

$$f(\theta) = L(\theta) = \sum (S_n \text{ Cos } n\theta + C_n \text{ Sin } n\theta) \qquad (4,3)$$

In this expression, the S_n, C_n are the coefficients to be determined by the following relations:-

$$S_n = \frac{2}{\pi} \int_0^{\pi} L(\theta) \text{ Cos } (n\theta)\, d\theta \tag{4,4}$$

$$C_n = \frac{2}{\pi} \int_0^{\pi} L(\theta) \text{ Sin } (n\theta)\, d\theta \tag{4,5}$$

Equation (4,2) is expanded as follows:-

$$\begin{aligned} L_A &= \sum A_n \,(\text{Sin } n\theta \text{ Cos } \phi_n + \text{Cos } n\theta \text{ Sin } \phi_n) \\ &= \sum ((A_n \text{ Sin } \phi_n) \text{ Cos } n\theta + (A_n \text{ Cos } \phi_n) \text{ Sin } n\theta) \\ &= \sum (\quad S_n \quad \text{Cos } n\theta + \quad C_n \quad \text{Sin } n\theta) \end{aligned} \tag{4,6}$$

wherein

$$\left.\begin{aligned} S_n &= A_n \text{ Sin } \phi_n \\ C_n &= A_n \text{ Cos } \phi_n \end{aligned}\right\} \quad \tan \phi_n = \frac{S_n}{C_n} \; ; \; A_n = \sqrt{S_n^2 + C_n^2} \tag{4,7}$$

The integrals referred to above in equations (4,4) and (4,5) are evaluated by a summation in 5° steps. Thus, (4,4) may be solved by using a Euler-Maclaurin expansion, expressed in the form

$$\int_0^{m\delta\theta} f(0)d\theta = \delta\theta \,(f(0) + f(\delta\theta) + f(2\,\delta\,\theta) + \ldots \; f(m-1)\,\delta\,\theta)$$

where $f(\theta) = L(\theta)\text{Cos}(n\theta)$, $m\delta 0 = \pi$; $\delta\theta$ is the step size and m is the number of steps. The summation was performed in the Fortran Programme.

The advantage of this method lies in the fact that the origin of the torque curves may be taken at the left hand side of the trace. The quantity A_n contains all the information about the amptitude of the Fourier Coefficient required in this case.

Shear Correction

The form of the torque curves was discussed in Chapter 2. There it was noted that the curve traced out by the pen recorder was not described by equation (1,5).

Using equation (2,1) the angle at which the torque which was traced out should have occurred in order to agree with (1,5) may be found by adding or subtracting the shear correction, depending on the nature of the torque curve. In order to perform this task reasonably efficiently, the shear angle was calculated for the value of field used in obtaining a given trace, and for a given torque.

Using the equivalence of one degree per millimetre on the X-axis of the trace, the shear angle was converted to millimetres. The torques then had to be moved this distance to obtain the true abscissa for equation (1,5).

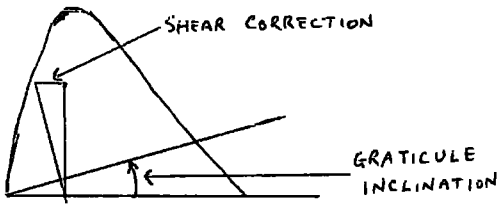

Fig.(4,1)
RELATIONSHIP OF SHEAR CORRECTION AND GRATICULE INCLINATION

Fig. (4,1) attempts to illustrate the conversion of the shear correction to a graticule inclination. If the graticule is tilted relative to the X-axis in a direction such as that indicated in Fig. (4,2), here is a method of reading the curves.

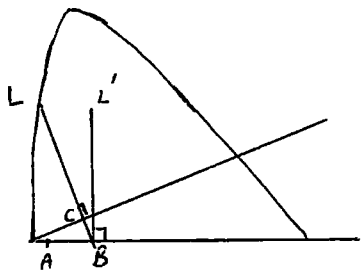

Fig.(4,2)
INCLINATION OF GRATICULE

The torque, L, which is recorded at A, should occur at B for equation (1,5) to be valid. The distance AB is evaluated from θ, equation (2,1) expressing θ in millimetres.

Then, the inclination of the graticule which is required to project the measured torque to the correct abscissa point is found as the angle L B L'.

To make it easier, the distance between the 17.5 cm mark on the inclined graticule and the axis of the trace is made to be:-

$$17.5 \tan (L\ B\ L')$$

Provided the quantity $\frac{\mu_o L}{B_o M_s V}$ is small, then $\theta \propto L$ (equation 2,1); and this is the justification for inclining the graticule.

In practise, the length CL was read off from the trace; the variable length BC, Fig. (4,2), was added to it and the total length BL projected to the ordinate BL'. The process was carried out on the computer.

Some Shear Correction Values

The following calculations are based upon:-

Magnetometer calibration constant	1.24×10^{-2}	Nm V^{-1}
Pen recorder scale factor	10^{-2}	V cm^{-1}
Sample volume	$1{\cdot}742 \times 10^{-8}$	m^3
Saturation magnetization of Nickel	0·606	Tesla
μ_o	$4\pi \times 10^{-7}$	N A^{-2}
Torque curve trace height	4·0	cm

Shear angle $\theta = \text{Sin}^{-1} \frac{\mu_o L}{B_o M_s V}$

$$\theta = \text{Sin}^{-1} \frac{0{\cdot}059}{B_o}$$

and assume 1^o = 1 mm on trace.

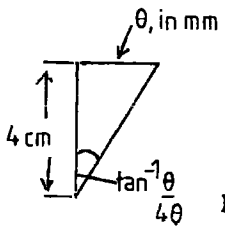

Fig. (4,3)

TABLE (4,1)

Electromagnet Current Amps	Applied field Tesla	θ^o	"DY"= 17.5 $\tan^{-1} \frac{(\theta(mm))}{(40\ mm)}$
10	0.26	13.12	5.74
20	0.505	6.71	2.94
30	0.635	5.33	2.33
40	0.715	4.73	2.07

Electromagnet Current Amps	Applied field Tesla	θ°	"DY"= 17.5 $\tan^{-1}\left(\frac{\theta(mm)}{40mm}\right)$
50	0.76	4.45	1.95
60	0.81	4.18	1.83
70	0.855	3.96	1.73
80	0.89	3.80	1.66
90	0.925	3.66	1.60
100	0.96	3.52	1.54
110	0.99	3.42	1.50
120	1.02	3.32	1.45

The parameter "DY" is the distance, measured along the graticule, from the 17.5 cm ordinate to the horizontal θ axis of the trace. It simply forms a convenient label for identifying the shear.

TABLE (4,2)

K_i Results, at $77^{\circ}K$, for nickel in the (110) plane

Magnetic field Tesla	"DY" cm	K_1 $10^3\ J\,m^{-3}$	K_2 $10^3\ J\,m^{-3}$	K_3 $10^3 J_m{}^{-3}$
0.635	-2.33	-76.3	-9.6	12
0.760	-1.95	-77.7	-4.2	9
0.86	-1.73	-80.0	4.7	4
0.96	-1.54	-81.1	8.7	1
1.01	-1.45	-81.7	10.4	-1

Franse's (1969) results are presented here for comparison:-

1.8	- - -	-84.2	8.3	-16.4

In another experiment, values of K_1 and K_2 were recorded for a range of values around a nominal "DY". This was done to see how sensitive K_1 and K_2 were to change in " DY". It also provided an estimate of the possible error from the estimate of shearing.

TABLE (4,3)

The Dependence of K_1 on "DY" at 77°K.

Magnetic field (Tesla)	"DY" (cm)	K_1 (10^3 J m^{-3})	K_2 (10^3 J m^{-3})
0.76	-1.1	-73.3	-28.8
	-1.5	-77.2	- 7.64
	-1.7	-76.4	-12.1
	-1.75	-76.3	-12.1
	-1.9	-77.2	- 5.9
	-2.1	-78.8	3.77
0.96	-1.3	-79.0	- 6.17
	-1.6	-82.6	17.0
	-1.8	-84.1	19.6
	-1.9	-84.3	30.5
	-2.0	-83.2	20.9
	-2.25	-83.2	33.1
1.01	-0.75	-96.8	71.9
	-0.5	-76.4	-26.4
	-0.85	-78.0	-14.4
	-1.0	-76.6	-27.9
	-1.2	-82.7	21.0
	-1.6	-82.3	16.1

Conclusions

From the K_1 results presented at 77°K it would appear that there is a magnetic field-anisotropy dependence. This is despite the fact that the K_2 are highly dependent on the nature of the shearing correction - for by applying the standard method indicated, K_1 appears to be approaching the value quoted by Franse. However the value of K_2 disagrees significantly with that of Franse, but appears to have an increasing value with applied field. See Fig. (4,4).

APPLIED MAGNETIC FIELD VARIATION
OF K_1, K_2 AND K_3
IN (110) PLANE AT 77K.

Fig.(4,4)

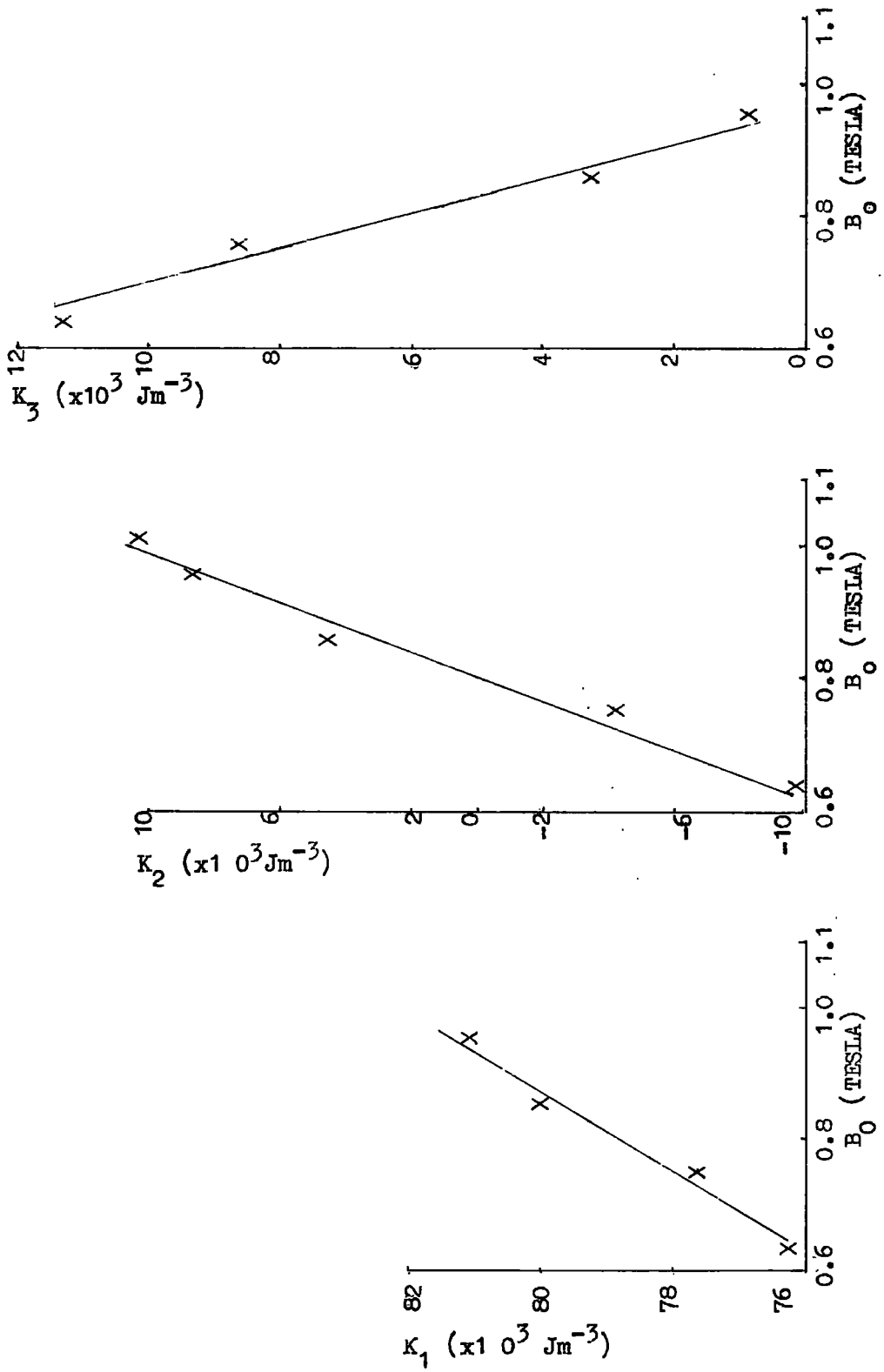

Secondly, the value of K_1 is stable relative to other parameters being varied, as shown by the variable "DY". However, K_2 is very variable, and the only reliable method of evaluating it in the present conditions is to define the shearing conditions as exactly as possible.

Evaluation of K_3 gives no agreement with other workers, and this value must be highly suspect. This is because the Fourier Coefficient required to evaluate K_3 is that of the 6θ component, and this coefficient was in most cases at least an order of magnitude smaller than the Fourier Coefficients of the 2θ and 4θ components. When attempting to measure the trace of the pen recorder, the accuracy of measurement is at best, about 2 mm; and often much worse. The output would need to be magnified by 10 times to render the 6θ component measurable, and this would cause the pen to go off scale.

Estimate of error in (110) plane

Major sources of error are:-

Slight misorientation of the inclined graticule - as reflected in the value of "DY".

Error in reading the torque ordinates from the trace.

The misorientation can be observed through table (4,3) for K_1 and K_2 and it can be seen that for K_1 error due to misorientation is just over ± 2% maximum. For K_2 this error is seen to be very much larger, over 100% in some cases eg.0.96 Tesla.

The error in reading the torque trace is thought to be interpretable by considering the amplitude of the Coefficient of Sin (6θ). The largest value obtained, in connection with table (4,2) was $5.36 \times 10^{2} J\,m^{-3}$ which represents about 1 mm on the trace. Noise on the trace made reading to this accuracy impossible. Thus, this coefficient is more likely to be just random error from trace reading.

Measurement of K_1 in the (100) plane

The torque curves derived from experiments in the (100) plane were analysed by simply halving the peak to peak value of the trace.

In accordance with equation (1,6) this amplitude represents the Coefficient of Sin (4θ); and if K_3 is ignored in a first approximation, since it is very much smaller than K_1, the amplitude may be used to determine K_1. The results for the two nickel samples are shown in Figs. 4,5 and 4,6 for a range of temperatures from 15K to 293K. Amighian's results are also recorded there for ease of comparison.

Measurement of Resistivity

A simple calculation, based on equation (3,1) gave the resistivity results down to a temperature at which the voltage across the sample was below the resolving power of the digital voltmeter. The variation of resistivity with temperature for the two samples investigated is shown in Figs. (4,7 and 4,8).

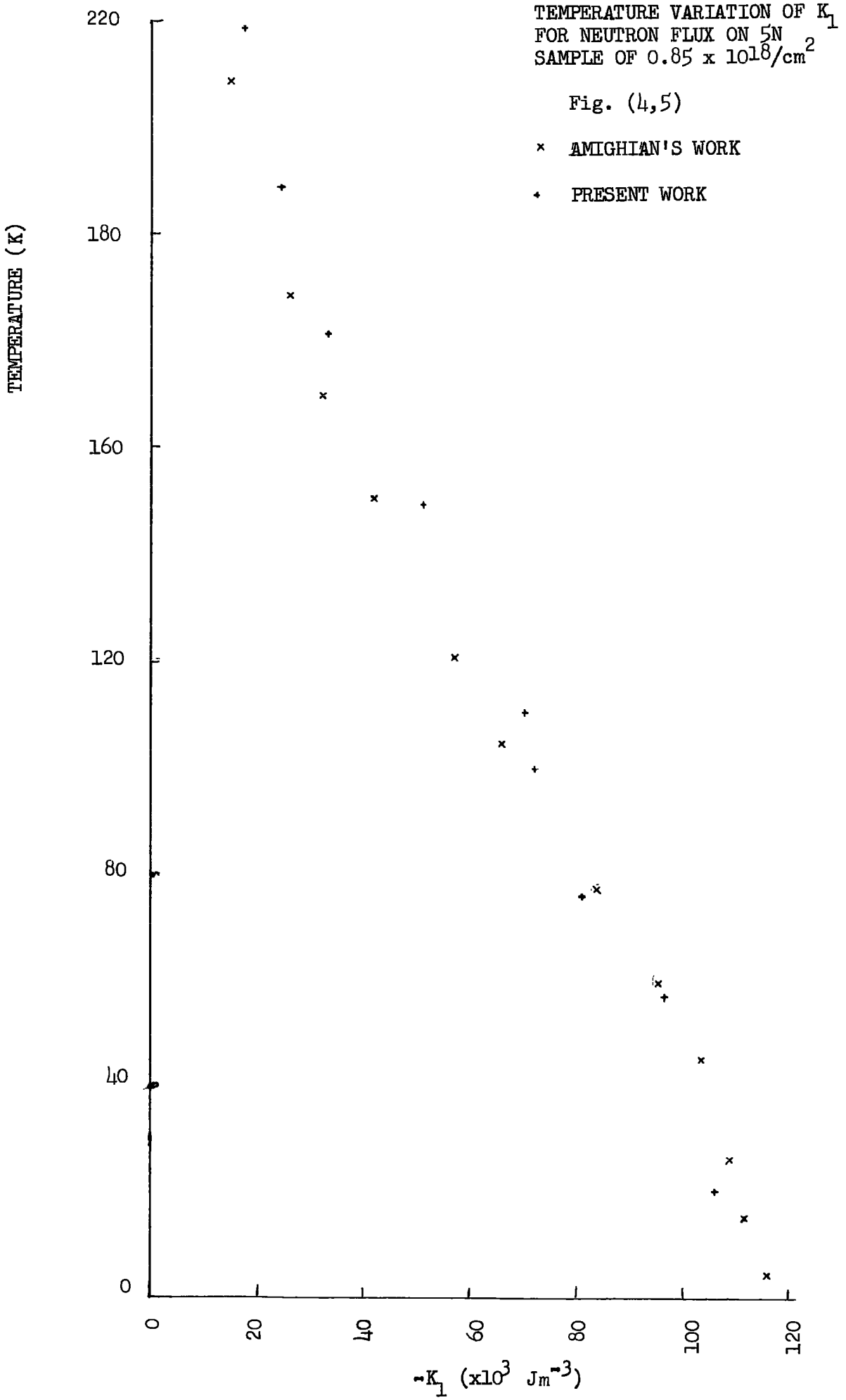
TEMPERATURE VARIATION OF K_1
FOR NEUTRON FLUX ON 5N
SAMPLE OF 0.85 x $10^{18}/cm^2$
Fig. (4,5)
× AMIGHIAN'S WORK
+ PRESENT WORK
TEMPERATURE (K)
220
180
160
120
80
40
0
0
20
40
60
80
100
120
$-K_1$ ($x10^3$ Jm^{-3})

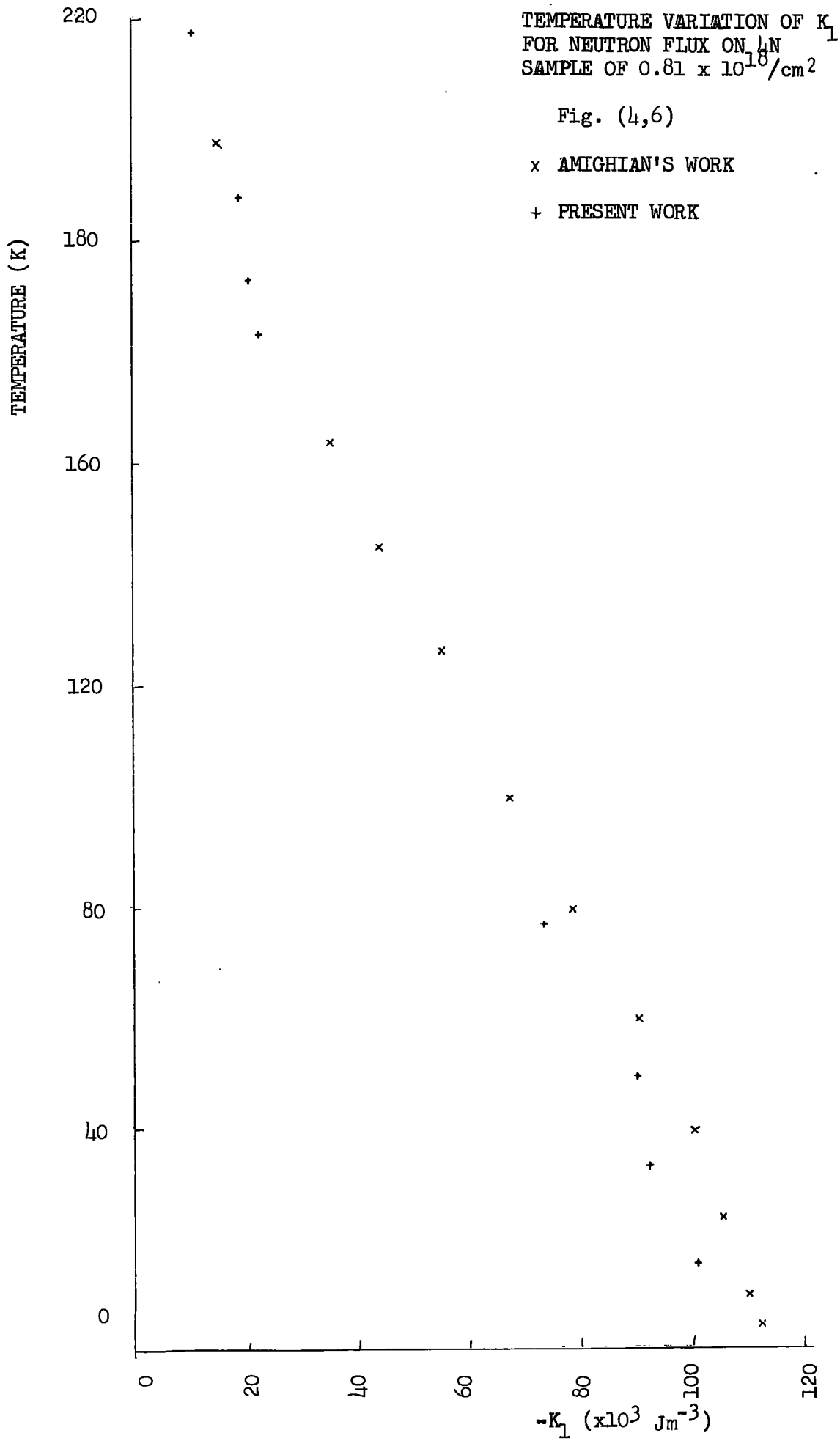
TEMPERATURE VARIATION OF K_1
FOR NEUTRON FLUX ON 4N
SAMPLE OF 0.81 x $10^{18}/cm^2$
Fig. (4,6)
x AMIGHIAN'S WORK
+ PRESENT WORK
TEMPERATURE (K)
220
180
160
120
80
40
0
0
20
40
60
80
100
120
$-K_1$ (x10^3 Jm^{-3})

TEMPERATURE VARIATION OF RESISTIVITY FOR NEUTRON FLUX ON 5N SAMPLE OF $0.85 \times 10^{18}/cm^2$

Fig. (4,7)

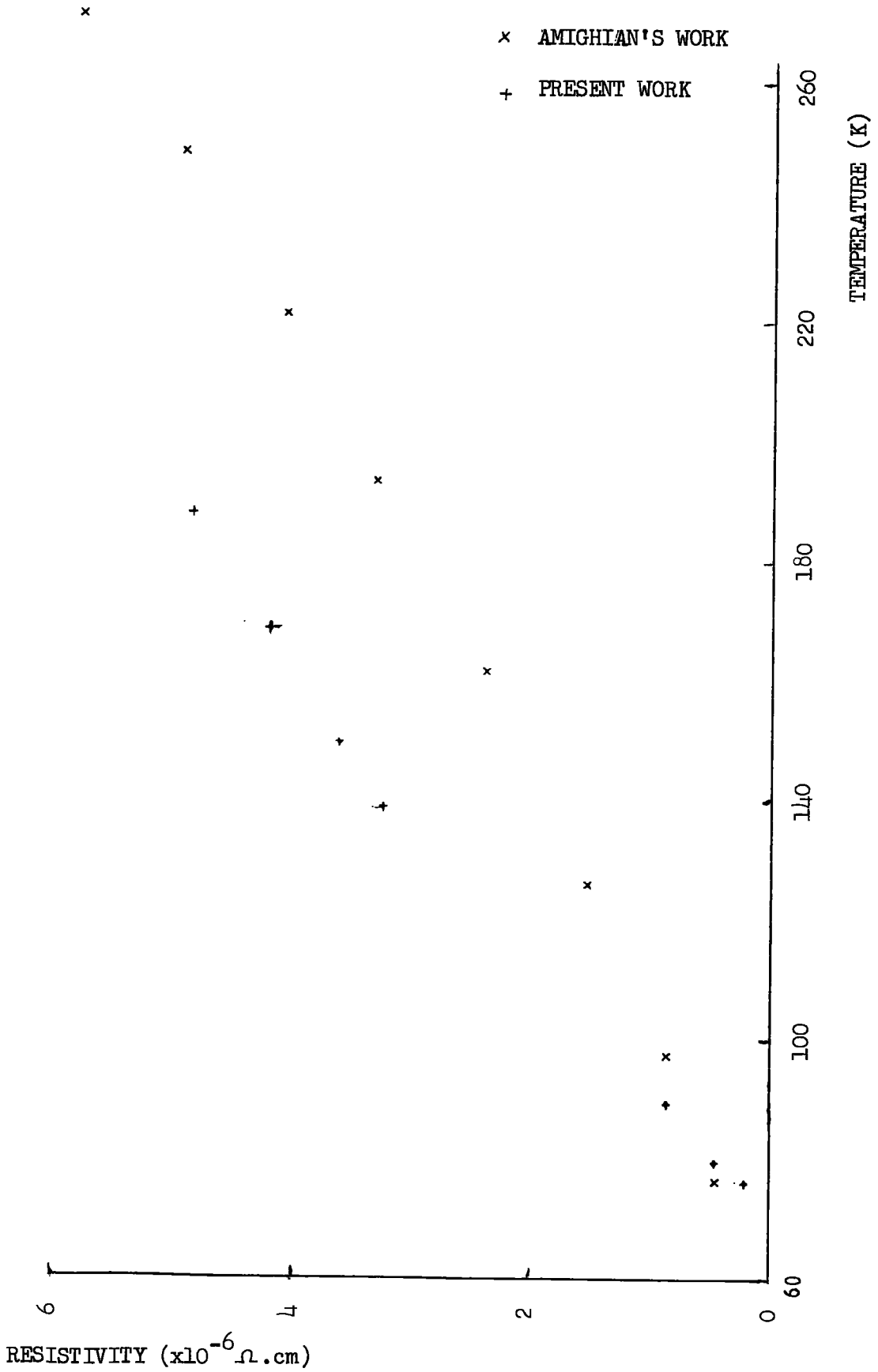

TEMPERATURE VARIATION OF RESISTIVITY FOR NEUTRON FLUX ON 4N SAMPLE OF

$0.81 \times 10^{18}/cm^2$

Fig. (4,8)

× AMIGHIAN'S WORK

\+ PRESENT WORK

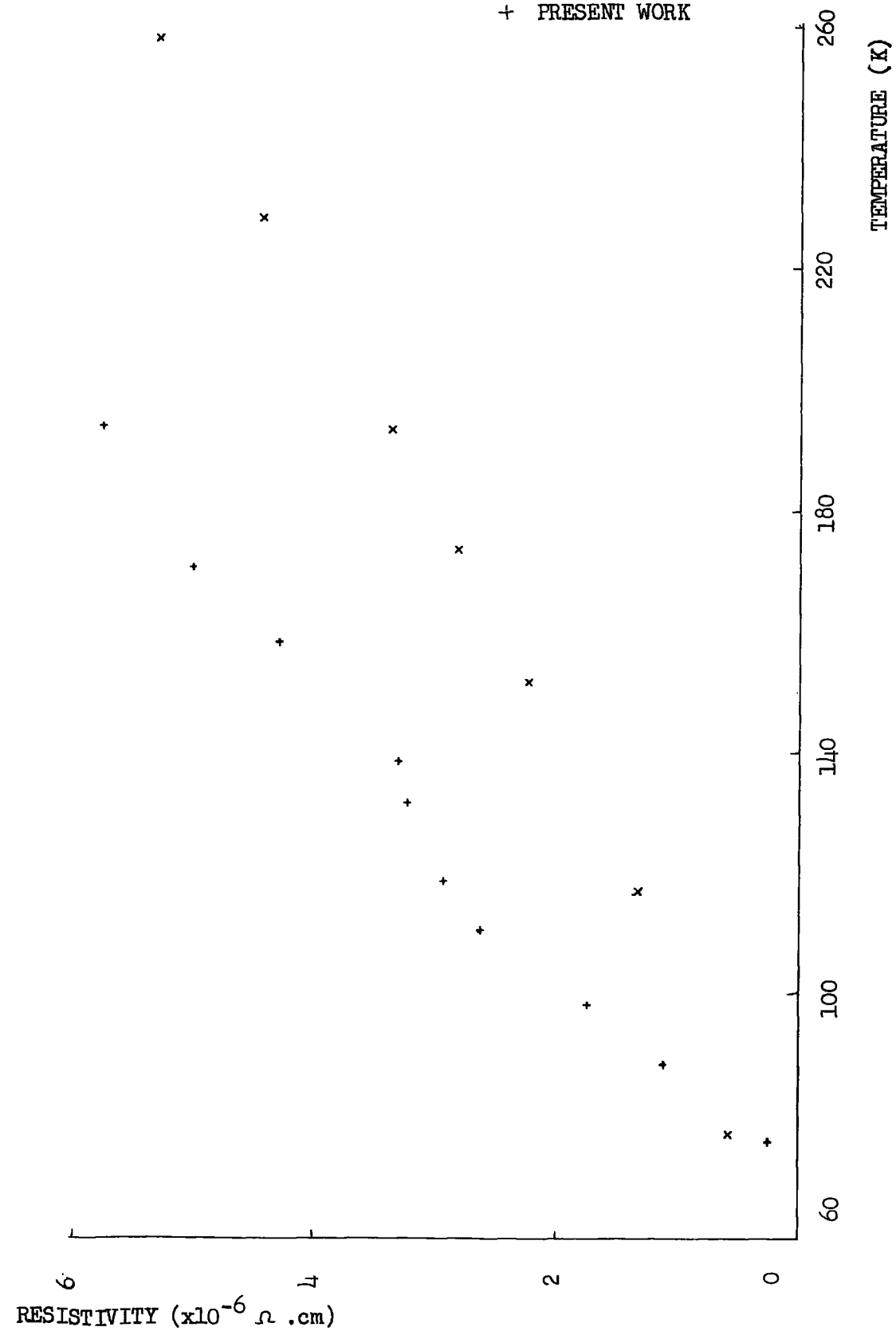

Chapter 5

Conclusions and Suggestions

CONCLUSIONS

(110) Plane Measurements

The first anisotropy constant, K_1, for nickel in the (110) plane can be measured by torque magnetometry. A graph of K_1 against external field is plotted in Fig. (4,4). The error in the measurement is estimated to be about 2%.

The second anisotropy constant, K_2, can also be measured, and measurements are recorded in Fig. (4,4). K_2 is very sensitive to graticule orientation.

The third anisotropy constant, K_3, was below the resolving power of the apparatus.

The precise orientation of the measuring graticule is important as indicated in table (4,3).

K_1 Variation with "concentration" in (100) plane

No significant difference was found between the K_1 variation with temperature for either 5N or 4N single crystal nickel spheres which had been irradiated with 8.5×10^{17} neutrons cm^{-2} and 8.1×10^{17} neutrons cm^2 respectively, as shown in Figs. (4,5) and (4,6).

No significant difference was found between the residual resistivity for either 5N or 4N nickel bars irradiated with 8.5×10^{17} neutrons cm^{-2} and 8.1×10^{17} neutrons cm^{-2} respectively.

DISCUSSION AND RECOMMENDATIONS

Anisotropy Constants in (110) Plane

In order to measure K_3, the output of the apparatus must be sufficiently sensitive to record the 6θ component in the torque curve. A larger output

is certainly desirable. Since the torque measured is that which is required to balance the magnetization (magnetic moment per unit volume) - crystallographic direction interaction, increasing the physical size of the specimen would increase the torque and hence increase the Fourier components.

As well as increasing the size of the specimen, the noise from the electronics could be eliminated. This would yield a smooth torque curve, allowing the 6θ component to be measured with greater certainty.

K_1 Variation with "concentration" in (100) plane

It may be that the radiation damage had annealed out of the samples during storage. More irradiations could be carried out, over a greater range of doses and the measurements performed immediately. Such a procedure raises problems regarding the handling of radioactive material. In this connection it should be noted that the maximum permissible dose for a non-registered worker is 1.5 mrem hr^{-7}; and that this dose is based upon 40 hours $week^{-1}$ for 50 weeks yr^{-1} spent continuously working with the material. The reaction of a contamination monitor ought to be interpreted in this context when deciding whether or not the material is safe to handle. Of course, the expert advice of the radiological protection officer should be sought as a matter of legal necessity.

A method of inducing damage thermally may be considered. Samples could be heated to allow atomic migration and then quenched to maintain the internal damage so caused. Resistivity measurements could be made to monitor the amount of damage. The procedure is safer than irradiation.

Resistivity

Using the arrangement described earlier, it was found that below 60K the voltage measurements necessary to determine the resistivity became unobservable. A more sensitive detection system seems desirable, the most well known being a phase sensitive detector, in order that small changes can be accurately monitored.

In the present investigation, the results were compared with those of Amighian so that there was little point is using more sensitive apparatus than he had used.

The observation that the crystal had been affected by the bombardment could be made because it was radioactive. Since the residual resistivity was unchanged, the electronic mean free path was unaltered. The anisotropy was also found to be unaltered. That they were "unaltered together" in spite of some crystal damage gives "moral" support to the hypothesis tested.

APPENDIX I

Programme for Fourier Analysis

```
PAGE 0001  FTN.   4:17 PM  TUE.,  13  JUNE,  1978

 0001  FTN4,B,L
 0002        PROGRAM MSCJE (3,90),13,66,78 K(I) 110 PLANE
 0003        REAL AA(36,6),AB(36,6),AC(36,6),TA(36),ALPHA(6)
 0004        REAL FOUCPT(6),FOCPT1(6),A(6),S(6),C(6)
 0005        INTEGER TITLE(32),IN,OUT,PRAMS(5)
 0006        EQUIVALENCE(IN,PRAMS),(OUT,PRAMS(2))
 0007        CALL RMPAR(PRAMS)
 0008        IF(IN.LE.0)GO TO 999
 0009        IF (OUT.LE.0)OUT=IN
 0010        ITOF=OUT+1100B
 0011        CALL EXEC(3,ITOF,-1)
 0012  107   READ(IN,*)(TA(I),I=1,36)
 0013        READ(IN,*)DY
 0014        READ(IN,*)CAL,SCAL,RMASS
 0015        CALL REIO(1,IN+4000B,TITLE,-64)
 0016        CALL ABREG(ISTAT,LENTL)
 0017        CALL EXEC(2,OUT,TITLE,-LENTL)
 0018        SCAL=SCAL*0.001
 0019        RMASS=RMASS*0.000001
 0020        NCOUNT=5
 0021        CALL SP1(AA)
 0022        IF(OUT.EQ.6)CALL LURQ(1,6,1)
 0023        WRITE(OUT,11)NCOUNT
 0024    11  FORMAT(/"THE TORQUES FROM THE GRAPH ARE",I2," DEGREE STEPS "
 0025        WRITE(OUT,12)(TA(I),I=1,36)
 0026    12  FORMAT(10(F6.2))
 0027        WRITE(OUT,13)DY
 0028    13  FORMAT(/"DY = ",F5.2)
 0029        CALL SP4(TA,DY)
 0030        J=5
 0031        WRITE(OUT,14)J
 0032    14  FORMAT(/"SHEARED TORQUES AT",I2,"DEGREE INTERVALS")
 0033        WRITE(OUT,15)(TA(I),I=1,36)
 0034    15  FORMAT( 10F8.4)
 0035        DO 100 K=1,6
 0036        I=1
 0037   101  AB(I,K)=TA(I)*AA(I,K)
 0038        I=I+1
 0039        IF (I.LE.36) GO TO 101
 0040   100  CONTINUE
 0041        CALL SP5(AA)
 0042        DO 102 K=1,6
 0043        I=1
 0044   103  AC(I,K)=TA(I)*AA(I,K)
 0045        I=I+1
 0046        IF (I.LE.36) GO TO 103
 0047   102  CONTINUE
 0048        WRITE(OUT,16)CAL,SCAL,RMASS
 0049    16  FORMAT(//"MAGNETOMETER CALIBRATION FACTOR IS:",E10.3," NM/V"
 0050       C'              PEN RECORDER SCALE IS:,"E10.3," V/CM",/,
 0051       C'                    SAMPLE MASS IS:",E10.3," KG")
 0052        J=5
 0053        WRITE(OUT,17)J
 0054    17  FORMAT(//"RESULTS OF FOURIER ANALYSIS FOR ANGLE INCREMENTS",
 0055        WRITE(OUT,18)J
```

```
0056     18  FORMAT(//"COEFFS OF SIN N(THETA), FOR STEP SIZE",I2," >>JM(-
0057         CALL SP2 (AB,SUMI,M,I,FOUCPT,CAL,SCAL,RMASS,OUT)
0058         DO 104 M=1,6
0059         FOCPT1(M)=FOUCPT(M)
0060         C(M)=FOUCPT(M)*FOUCPT(M)
0061    104  CONTINUE
0062         WRITE(OUT,19)J
0063     19  FORMAT(//"COEFFS OF COS N(THETA) FOR STEP SIZE",I2," >>JM(-3
0064         CALL SP2 (AC,SUMI,M,I,FOUCPT,CAL,SCAL,RMASS,OUT)
0065         DO  105 M=1,6
0066         S(M)=FOUCPT(M)*FOUCPT(M)
0067         A(M)=SQRT(S(M)+C(M))
0068         ALPHA(M)=(180.0/3.14159)*ATAN(FOUCPT(M)/FOCPT1(M))
0069    105  CONTINUE
0070         A21=A(2)
0071         A41=A(4)
0072         A61=A(6)
0073         WRITE(OUT,20)
0074    20   FORMAT(///"RESULTS OF ANALYSIS WITH PHASES")
0075         DO 106 M=2,6,2
0076         WRITE(OUT,21)M,J,A(M),ALPHA(M)
0077      21 FORMAT(/"COEFF. OF",I2," THETA CPT, FOR",I2," DEG. STEPS IS
0078        CE10.3,/,"PHASE ANGLE IS ",E10.3)
0079    106  CONTINUE
0080         WRITE(OUT,23)A21,A41
0081     23  FORMAT(/" A2 = ",E10.3," A4 = ",E10.3)
0082         A21=(-64.0*A21)
0083         A41=(-16.0*A41)
0084         A61=64.0*A61
0085         D=10.0
0086         DK1=(A21-A41)
0087         DK2=(16.0*A41-6.0*A21)
0088         A21=2.0*A21
0089         A41=8.0*A41
0090         A61=2.0*A61
0091         DK3=32.0*(8.0*A61-6.0*A41)-2.0*48.*A61+A21*48.*6.
0092         RK1=DK1/D
0093         RK2=DK2/D
0094         RK3=DK3/1344.0
0095         WRITE(OUT,26)DY
0096     26  FORMAT(//"ANISOTROPY CONSTANTS,K(I),FOR DY =",F5.2," ARE:-"
0097         WRITE(OUT,24)RK1,RK2,RK3
0098     24  FORMAT(/"K1 = ",E10.3," JM(-3)",/,"K2 = ",E10.3," JM(-3)"
0099        C,/,'K3 = ",E10.3," JM(-3)")
0100         CONTINUE
0101         WRITE(OUT,25)
0102     25  FORMAT( " END OF DATA INPUT")
0103         CALL EXEC(3,ITOF,-1)
0104    999  STOP
0105         END
FTN4 COMPILER: HP92060-16092 REV. 1726
```

```
0106          SUBROUTINE SP1(AA)
0107          REAL AA(36,6)
0108          DO 1 M=1,6
0109          DO 1 I=1,36
0110          K=I-1
0111      1   AA(I,M)=SIN(K*M*5.0*3.1416/180.0)
0112          RETURN
0113          END

0114          SUBROUTINE SP2(AA,SUMI,M,I,FOUCPT,CAL,SCAL,RMASS,OUT)
0115          REAL AA(36,6),FOUCPT(6)
0116          INTEGER OUT
0117          DO  1 M=1,6
0118          CALL SP3 (AA,M,SUMI,FOUCPT)
0119          J=5
0120          FOUCPT(M)=FOUCPT(M)*CAL*SCAL*8.9E3/RMASS
0121      1   CONTINUE
0122          DO 2 M=2,6,2
0123          WRITE(OUT,3)M,J,FOUCPT(M)
0124      3   FORMAT( " COEFFICIENT FOR",I2," THETA, FOR STEP SIZE",I2,
0125         C' IS',E11.4)
0126      2   CONTINUE
0127          RETURN
0128          END

0129          SUBROUTINE SP3 (AA,M,SUMI,FOUCPT)
0130          REAL AA(36,6),FOUCPT(6)
0131          I=1
0132          SUMI=0.0
0133      1   SUMI=SUMI+AA(I,M)
0134          I=I+1
0135          IF (I.LE.36) GO TO 1
0136          FOUCPT(M)=SUMI*5.0*2.0/180.0
0137          RETURN
0138          END
0139          SUBROUTINE SP4 (TA,DY)
0140          REAL TA(36)
0141          I=1
0142          R=0
0143      1   TA(I)=(TA(I)+R*DY/35)*COS(ATAN(DY/17.5))
0144          I=I+1
0145          R=R+1
0146          IF (I.LE.36) GO TO 1
0147          RETURN
0148          END
FTN4 COMPILER: HP92060-16092 REV. 1726
**  NO WARNINGS **  NO ERRORS **   PROGRAM = 00084       COMMON = 00000
```

```
PAGE 0000  FTN.    4:17 PM  TUE., 13  JUNE, 1978

 0149          SUBROUTINE SP5 (AA)
 0150          REAL AA(36,6)
 0151          DO 1 M=1,6
 0152          DO 1 I=1,36
 0153          K=I-1
 0154     1    AA(I,M)=COS(K*5.0*M*3.1416/180.0)
 0155          RETURN
 0156          END
FTN4 COMPILER: HP92060-16092 REV. 1726
**  NO WARNINGS **  NO ERRORS **   PROGRAM = 00071       COMMON = 00000
```

APPENDIX II

A Programme for the Removal of Neutron Irradiated Nickel Samples

The samples were contained in a small envelope of black plastic, wrapped round with Cadmium foil, contained in a plastic bottle which was packed in a metal tin marked "Radioactive". This was placed in a standard box of known dimensions.

The metal tin was opened with a tin opener under constant rate-meter monitoring and the plastic bottle was removed with the particulate packing. On opening the bottle, the Cadmium was seen to be radioactive, it was removed leaving the nickel samples in the black plastic packaging. No contamination of the packing (particulate matter) had occured.

The black plastic was broken and all fragments were recovered. The separate pieces, together with the Cadmium were placed in separate specimen bottles and radioactivity warning labels were stuck on.

Fill four specimen bottles, of a similar type to those holding the samples at present, with chloroform to about half fill each bottle. Place a lid on each bottle.

In a controlled radiation area and in a fume cupboard, open the two specimen bottles which hold the specimens.

Pour in liquid chloroform, sufficient to immerse the samples and replace the lids of the bottles.

Observe when the plastic is dissolved (how long this will take is not known).

Remove the lids from the second bottles of chloroform (having placed warning labels on them).

Remove the lids from the bottles containing the samples and, using tweezers, remove the samples and place them in the second bottles of chloroform. Replace the lids on each bottle of chloroform.

Repeat this process until as much of the plastic as possible has been removed.

When this condition has been fulfilled, dry the samples with a hair dryer, or in air, holding them with tweezers.

Place the samples in small sample bottles packed lightly with cotton wool and marked with radioactivity warning labels.

Ensure that all bottles are properly sealed and bear the appropriate labels, and that they will be disposed of in the correct manner.

Obtain a labelled container containing nitric acid to a depth sufficient to immerse the nickel samples. Using tweezers, dip the samples in the acid, remove and set down on an absorbent surface.

Pick up the sample again using tweezers across a different diameter and immerse in nitric acid.

Repeat this process six times.

Seal the nitric acid container, dispose of the absorbent surface and wash in water, sealing the water vessel and labelling it radioactive.

Dip the specimens into labelled containers containing chloroform and then blow dry the specimens, sealing all containers.

Transfer the specimens back to the Physics Department and store in a safe area until required.

When required, remove the sample from the bottle, using tweezers and care. Mount the specimen on top of a small brass rod using soft wax.

Take a Laue photograph using a recommended exposure time (Amighian) of four minutes.

Change the orientation of the crystal.

Take another photograph.

Continue this process until the required orientation has been found.

A sample holder, which is designed to hold the sample in the experimental apparatus, is mounted on a bracket which can slide along the track which supports the goniometer and is attached to the X-ray generator.

The holder is brought into contact with the sample and durofix glue is applied to form an adhesive bond between the sample and the holder.

The sample holder is mounted in the goniometer and another photograph is taken to ensure correct orientation.

The sample and sample holder are then mounted in the torque magnetometer and a warning label is attached to the apparatus.

When the experiment is completed, remove the sample from the magnetometer, place in the specimen bottle and inform Supervisor or Dr. Thompson and remove to radioactive store.

APPENDIX III

Derivation of the Correct Form of the (110) Plane Torque Equation

Franse (1969, p22) writes:-

$$L_A = -K_1 S'(\ell mn) - K_2 P'(\ell mn) - 2K_3 S(\ell mn) S'(\ell mn) + \ldots \qquad (2,7)$$

wherein ℓmn are the Miller indices of the plane being considered

& $S = \ell^2 m^2 + m^2 n^2 + n^2 \ell^2$

also $P = \ell^2 m^2 n^2$

$S(110) = \frac{1}{4} \sin^4\theta + \sin^2\theta \cos^2\theta \qquad S'(110) = \frac{1}{4} \sin 2\theta (1 + 3 \cos 2\theta)$

$P(110) = \frac{1}{4} \sin^4\theta \cos^2\theta \qquad P'(110) = S'(110) \frac{1}{2} \sin^2\theta$

The derivation proceeds as follows:-

$$L_A = -K_1 S' - K_2 S' \frac{\sin^2\theta}{2} - 2K_3 SS'$$

$$= -S' \left(K_1 + \frac{K_2}{2} \sin^2\theta + 2K_3 S\right)$$

$$= -\frac{1}{4} \sin 2\theta (1 + 3 \cos 2\theta) \left(K_1 + \frac{1}{2} K_2 + 2K_3 \left\{\frac{\sin^2\theta}{4} + \cos^2\theta\right\} \sin^2\theta\right)$$

In contrast, Franse writes:-

$$L_A = -\frac{1}{4} \sin 2\theta (1 + 3 \cos 2\theta) \left\{K_1 + \left\{\frac{K_2}{2} + 2K_3\right\} \sin^2\theta + \ldots\right\} \qquad (2,9)$$

REFERENCES

Amighian, J., Corner, W.D., (1976) J.Phys.F., 6,L309

Amighian, J., Corner, W.D. (1977) I.E.E.E. Trans.Mag., 13,928

Aubert, G. (1968) J.App.Phys., 39,504

Aukulov, N. (1936) Z.Phys., 100,197

Brailsford, F. (1966) Physical Principles of Magnetism, Van Nostrand, London

Brenner, R. (1957) Phys.Rev., 107,1539

Brooks, H. (1940) Phys.Rev., 58,909

Callen, E., Callen, H.B. (1960) J.Phys.Chem.Solids, 16,310

Callen, H.B., Callen, E. (1966) J.Phys.Chem.Solids, 27,1271

Carr, W.J. (1957) Phys.Rev., 108,1158

Carr, W.J. (1958) J.Appl.Phys., 29,436

Farrell, T., Greig, D. (1968) J.Phys.C. (Proc.Phys.Soc) 1,1359

Fletcher, G.C. (1954) Proc.Phys.Soc., 67,505

Franse, J.J.M. (1969) Ph.D. Thesis

Franse, J.J.M., de Vries, G., Kortekaas, T.F.M. (1973) Proc.Int.Conf. on Mag. Moscow

Franse, J.J.M, de Vries, G., Physica, 39, 477 (1968)

Hausmann, K. (1970), Phys.Stat.Sol., 38,809

Hausmann, K., Wolf, M., (1971), J.de Phys.Supp. to Vol. 32,C1-539

Hausmann, K., Wolf, M., Mulle, H., (1971) Phys.Stat.Sol., (B), 45,K99

Keffer, F. (1955) Phys.Rev., 100,1692

Keffer, F., Oguchi, T. (1960) Phys.Rev., 117,718

Low, D., (1969) Adv. in Phys., 18,371

Mori, Nobus (1969) J.Phys.Soc.Japan, 27,30

Van Vleck, J.H. (1937) Phys.Rev., 52,1178

Van Vleck, J.H. (1959) J.Phys.Radium, 20,124

Welford, J. (1974) Ph.D.Thesis, Durham Univ. England

Zener, C. (1954) Phys.Rev., 96,1335

ACKNOWLEDGEMENTS

I wish to thank Professor Wolfendale for allowing me to enter the department and do the research.

I also wish to thank, most sincerely, Dr. Corner; without his sustained, patient, kind and good humoured assistance, the thesis would never have been completed.

Ron Smith also helped a great deal, especially with the experimental side of the work - without his assistance there would have been nothing to write. Also the torque magnetometer layout is derived from him.

There are also the technicians; Mr. Moulson and Mr. Scott who provided back-up assistance where necessary.

I am grateful to Dr. M. Heath of Nottingham University for making available the nickel disc.

Finally, there is Mrs. R. Culbert, who typed a difficult manuscript very well, and with great efficiency.